Electronic Supplementary Information

Close insights into the growth pattern of palladium nanocubes with controllable sizes

Jianzhou Wu[a], Jing Zhao[a], Hehe Qian[a], Lei Yue[b], Yongsheng Guo[a,], and Wenjun Fang[a,]**

[a] Department of Chemistry, Zhejiang University, Hangzhou 310058, China

[b] Institute of Nuclear Physics and Chemistry, China Academy of Engineering Physics, Mianyang 621900, China

*To whom correspondence should be addressed

E-mail: fwjun@zju.edu.cn (W. Fang); wjjw@zju.edu.cn (Y. Guo).

Calculation of Electrochemical Details for Typical Synthesis Procedure. The conditional reduction potential $E_{AA}^{'}$ for AA in equation 3 can be described as follows (modified from reference 35):

$$E_{AA}^{'} = 0.553 - \frac{RT}{F}\mathrm{pH} + \frac{RT}{F}\ln\frac{\left[AA_O^{-}\right]}{\left[AA_R^{-}\right]} + \frac{RT}{2F}\ln\frac{K_O}{K_R} - \frac{RT}{2F}\ln\frac{K_O + [H^+]}{K_R + [H^+]} \qquad \textbf{(S1)}$$

where $\left[AA_O^{-}\right]$ and $\left[AA_R^{-}\right]$ indicate the equilibrium concentrations of AA in oxidative and reductive states, respectively. K_O and K_R are the first dissociation constants of the oxidized and reduced AA, respectively. Because of its weak acidity, AA with the oxidative form can be considered as a monovalent acid, and the values of pK_O and pK_R are given as 9.0 and 4.17. Considering the dosage of AA and ignoring the influence of other ions, the initial pH of the reaction system is 2.82.

Under typical synthesis procedure, when the reduction process is complete, the equilibrium concentrations of $[PdCl_4]^{2-}$, Cl^-, $[AA_O]^-$, and $[AA_R]^-$ are calculated to be 1.00 ✕ 10^{-6}, 8.00 ✕ 10^{-2}, 2.00 ✕ 10^{-2}, and 1.41 ✕ 10^{-2} mol/L, respectively. Hence, the value of $E_{AA}^{'}$ is 0.306 V, and the conditional reduction potential for $[PdCl_4]^{2-}$/Pd is 0.534 V.

Calculation of the Mole Fraction of Br in a Pd Nanocube. Because of the close values of the size of Br^- (r_{Br}) and the distance of Pd (200) faces (0.5 a), we define $2r_{Br}$ to be equal to a for simplification. Hence, the value for lattice constant of Pd is a. For a Pd nanocube with edge length of n, the number of atoms on surfaces is N, and the total amount of Pd atoms in the cube is N_{Pd}

$$N = 2 \times 6 \times \left(\frac{n}{a}\right)^2 = \frac{12\,n^2}{a^2} \qquad \textbf{(S2)}$$

$$N_{Pd} = 4 \times (\frac{n}{a})^3 = \frac{4n^3}{a^3} \quad \textbf{(S3)}$$

According to Scheme 2, every two Pd atoms possess one Br^-, and the number of Br^- on cubic surface is N_{Br}.

$$N_{Br} = \frac{1}{2}N = \frac{6n^2}{a^2} \quad \textbf{(S4)}$$

Consequently, the mole fraction Br^- in Pd cube is χ.

$$\chi = \frac{N_{Br}}{N_{Pd}} = \frac{3a}{2n} \quad \textbf{(S4)}$$

DFT Calculations. To analysis the properties of different Pd low-index facets, First-principle DFT calculations were employed with the pseudo-potential plane-wave method. Three different facets with 5 layer atomic thickness, namely {100}, {110} and {111}, were cleaved and covered by a vacuum slab of 10 Å. The geometries are full optimized *via* generalized gradient approximation (GGA) with Perdew-Burke-Ernzerhof (PBE) approximation[1]. The *k*-point was defined at 2 × 2 × 1. The calculations of electron density maps (Scheme S1) were performed with CASTEP[2].

To study the physical adsorption behavior of Br^- onto the top layer of Pd {100} facet, classical grand canonical Monte Carlo (GCMC) simulations were applied through Adsorption Locator module[3, 4]. The simulations were performed with the standard universal force field (UFF) in the temperature range of 300–500 K. The Br^- was adsorbed onto the octahedral cavity (Scheme S2) with adsorption energy of -0.8863 kcal/mol.

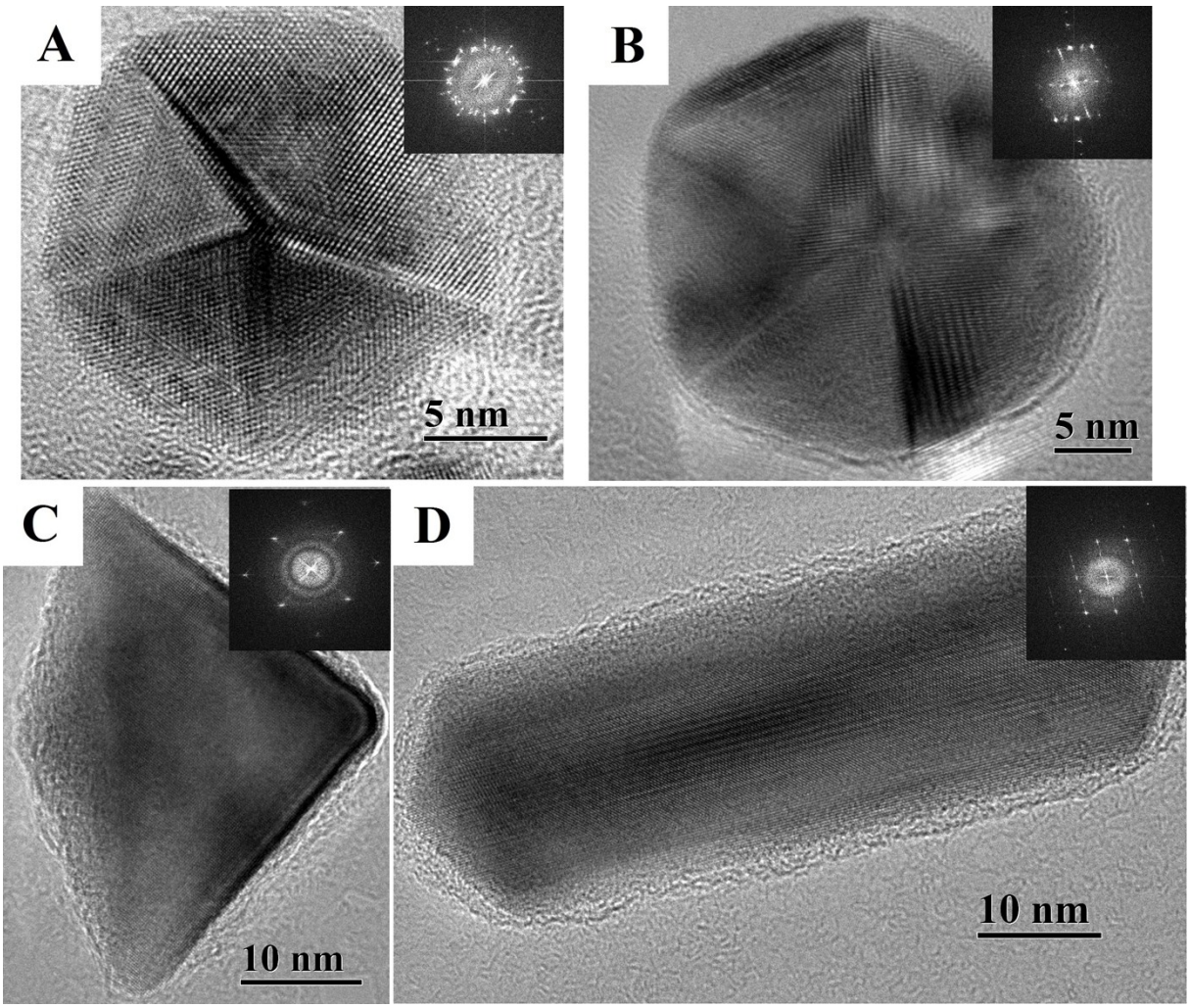

Fig. S1. HRTEM images of twinned crystals generated while preparing Pd nanocubes: (**A**) decahedron, (**B**) icosahedron, (**C**) triangular bipyramid and (**D**) pentagonal rod. Images inserted indicate the corresponding FFT pattern of each structure.

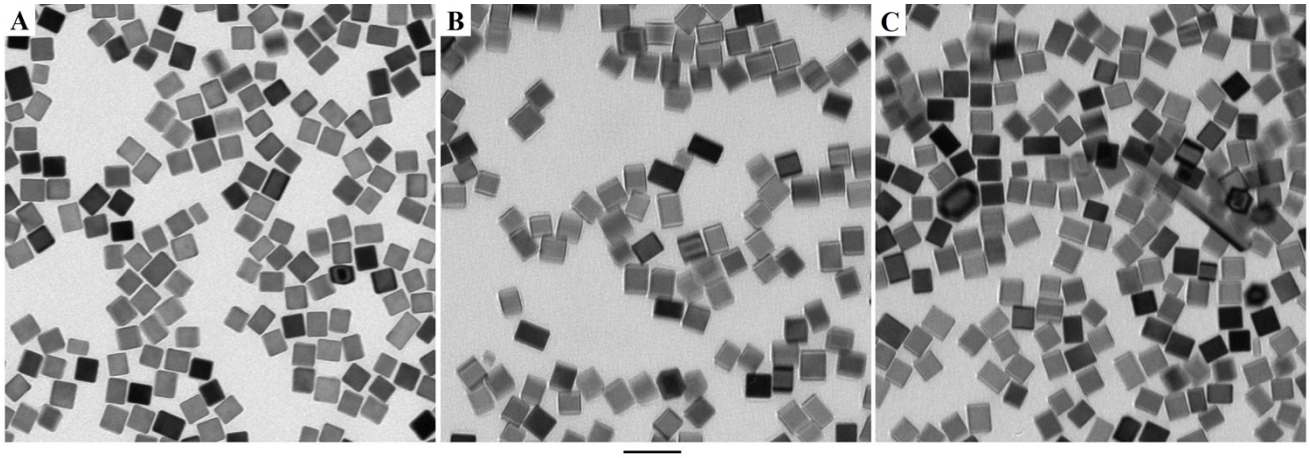

Fig. S2. TEM images of Pd nanocrystals reacted for (**A**) 3, (**B**) 7 and (**C**) 10 h under typical synthesis procedure. Scale bar: 50 nm.

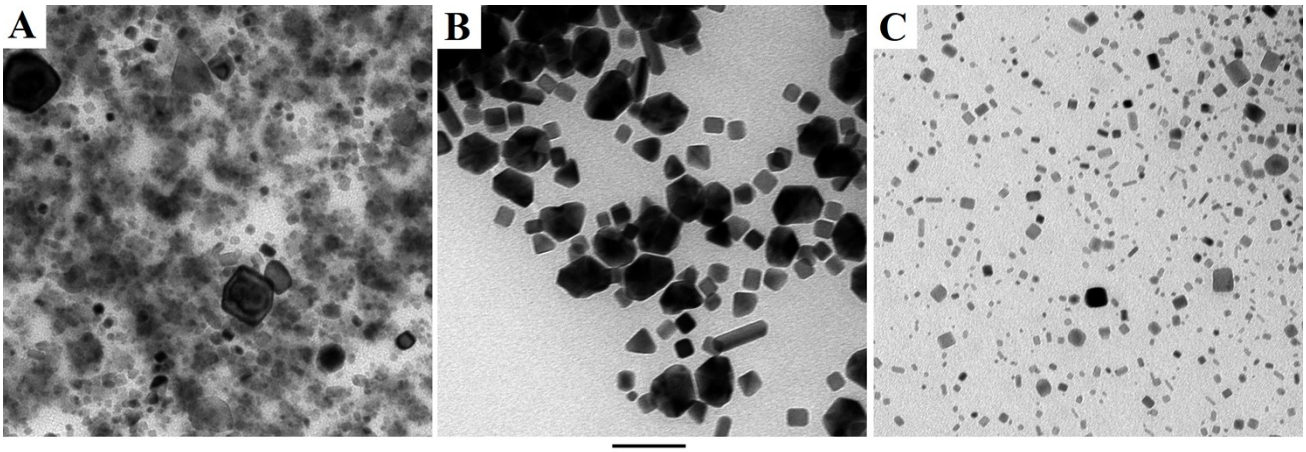

Fig. S3. TEM images of Pd nanocrystals prepared under typical synthesis procedure where KBr was replaced by same concentrations of (**A**) KI or (**B**) KCl, or same amount of (**C**) K_2PdBr_4 was occupied instead of K_2PdCl_4. Scale bar: 50 nm.

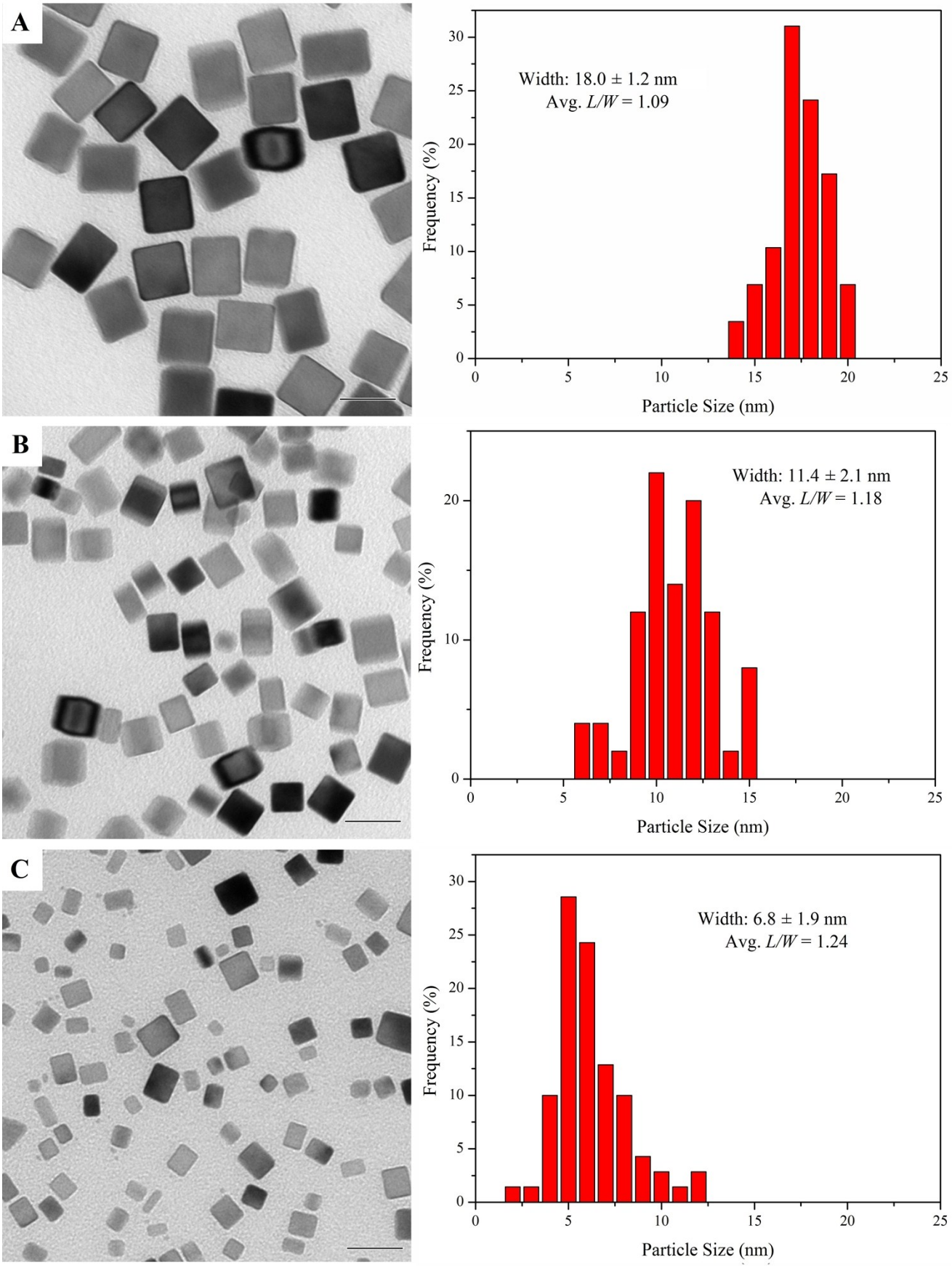
A
Width: 18.0 ± 1.2 nm
Avg. L/W = 1.09
Frequency (%)
Particle Size (nm)
B
Width: 11.4 ± 2.1 nm
Avg. L/W = 1.18
Frequency (%)
Particle Size (nm)
C
Width: 6.8 ± 1.9 nm
Avg. L/W = 1.24
Frequency (%)
Particle Size (nm)

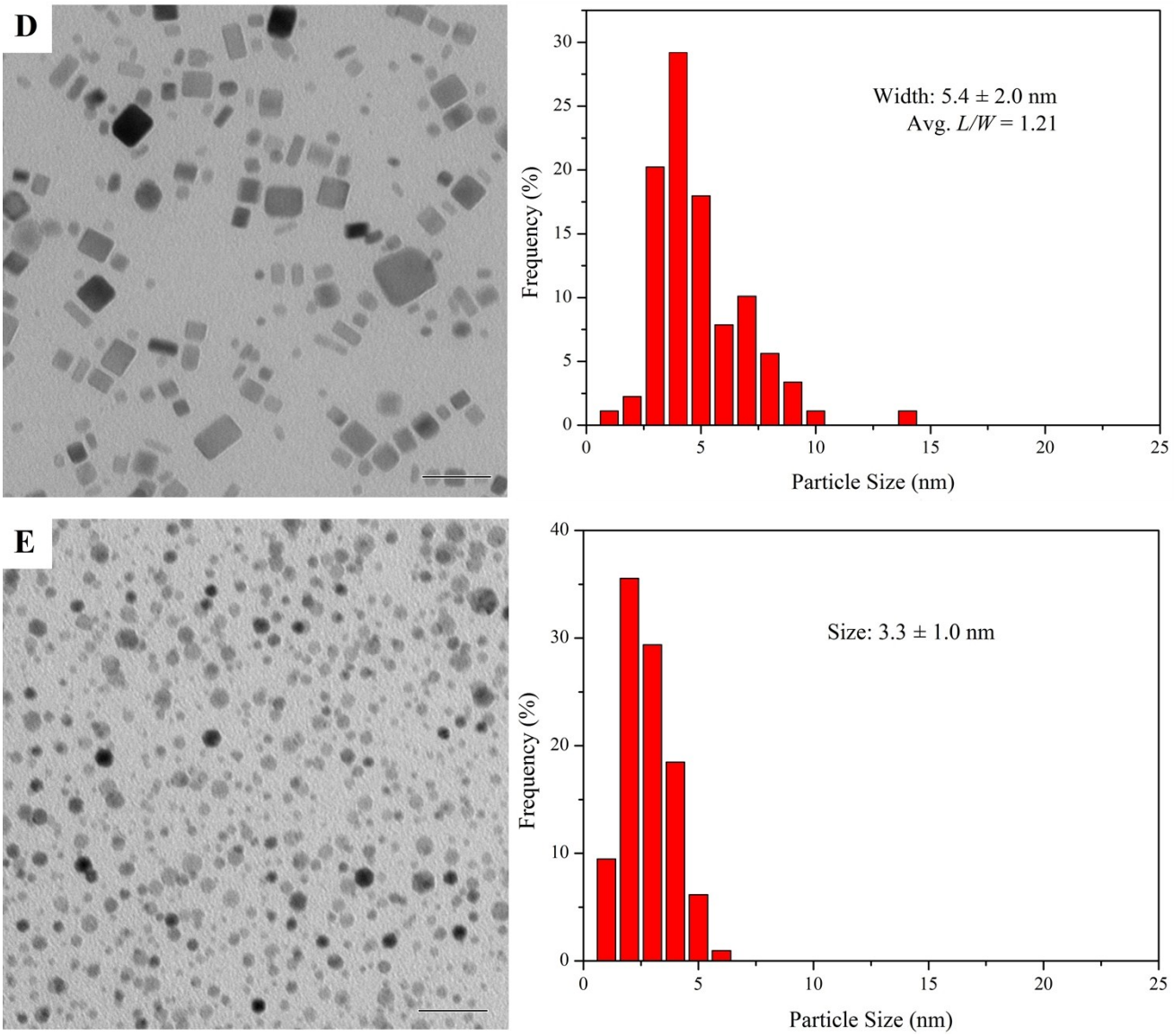

Fig. S4. TEM images of Pd nanostructures obtained with different concentrations of KBr (mmol/L): (**A**) 630, (**B**) 315, (**C**) 158, (**D**) 78.8 to (**E**) 0. Scale bar: 20 nm. (Width: the mean width of nanostructures; Avg. *L/W*: the average aspect ratio.)

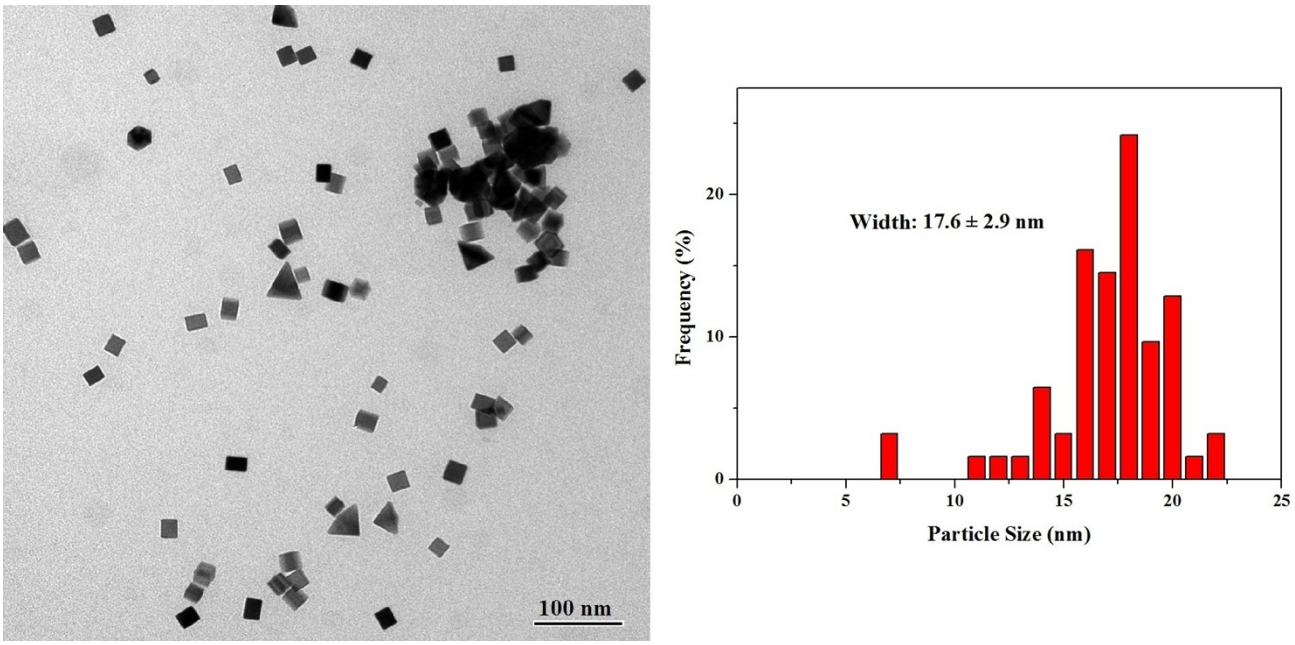

Fig. S5. TEM image and size distribution of Pd nanocubes gained with the concentration of KBr at 1.26 mol/L.

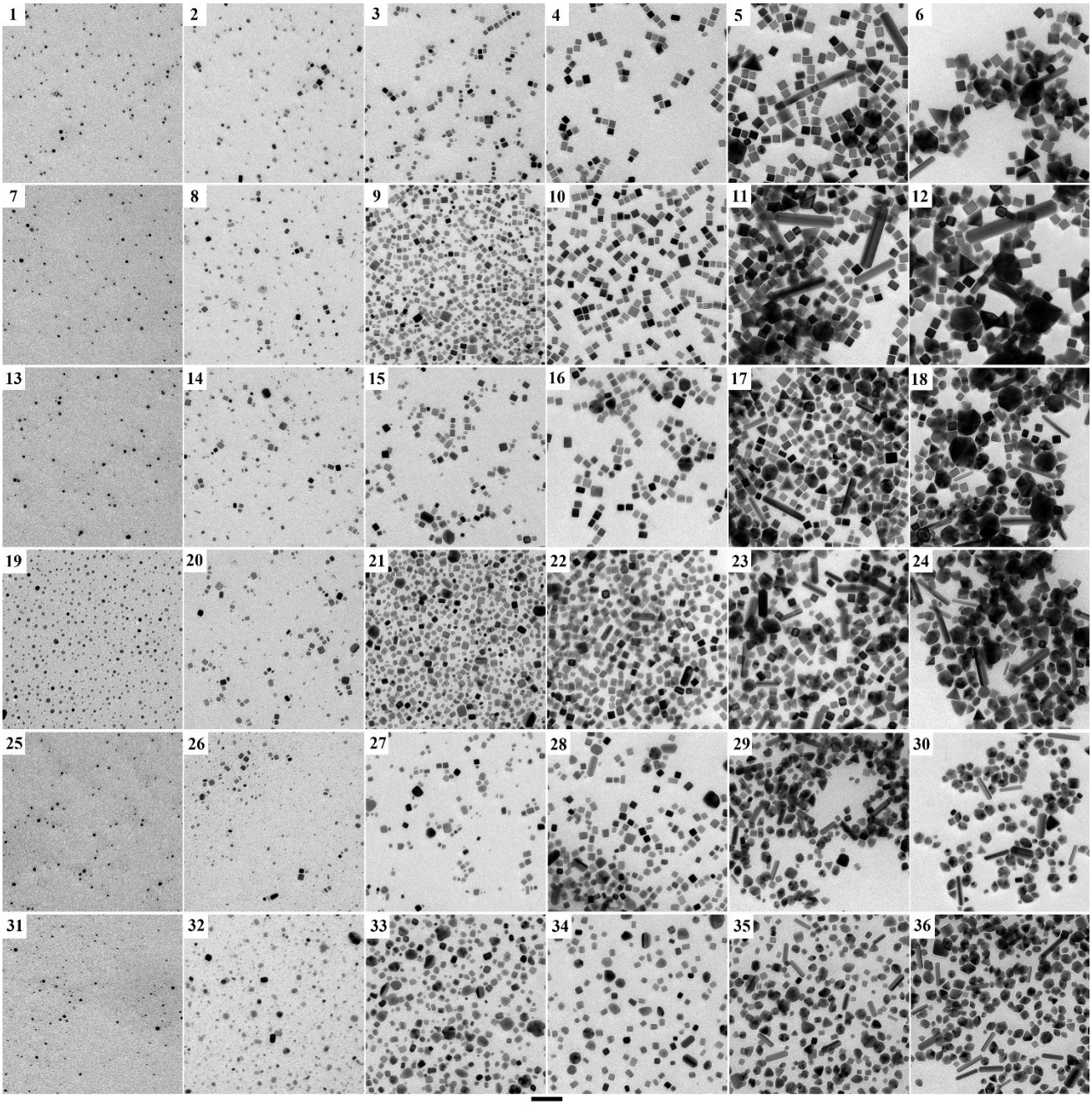

Fig. S6. TEM images of as-synthesized Pd nanoparticles based on the concentrations of reagents in Table S1 with AA as reducing agent and KBr as capping agent. Scale bar: 50 nm.

Table S1. Reagent concentrations for each reaction.

Items		Dosage of KBr / mmol/L					
		0	67.2	134	269	538	1.08×10^3
Dosage of AA / mmol/L	22.7	1	2	3	4	5	6
	45.4	7	8	9	10	11	12
	90.8	13	14	15	16	17	18
	182	19	20	21	22	23	24
	363	25	26	27	28	29	30
	728	31	32	33	34	35	36

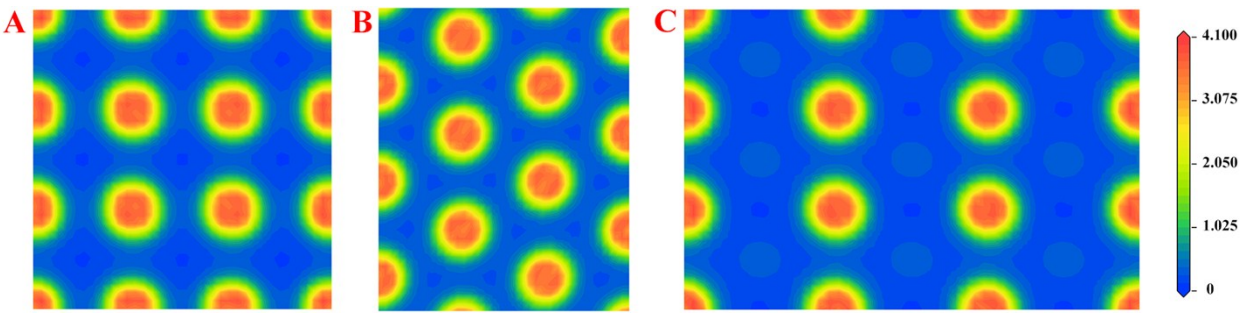

Scheme S1. Electron density map of (**A**) {100}, (**B**) {111} and (**C**) {110} Pd facets gained through primary DFT calculation.

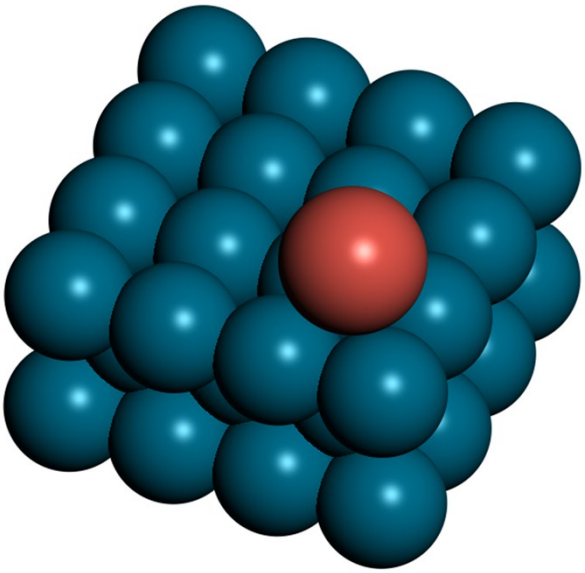

Scheme S2. Schematic illustration of one Br^- adsorbed onto Pd {100} facet.

REFERENCES

1. J. P. Perdew, K. Burke and M. Ernzerhof, *Phys. Rev. Lett.*, 1996, 77, 3865-3868.

2. S. J. Clark, M. D. Segall, C. J. Pickard, P. J. Hasnip, M. I. Probert, K. Refson and M. C. Payne, *Zeitschrift für Kristallographie-Crystalline Materials*, 2005, 220, 567-570.

3. D. Liu, H. Wu, S. Wang, Z. Xie, J. Li and W. Lin, *Chem. Sci.*, 2012, 3, 3032-3037.

4. S. S. Rath, N. Sinha, H. Sahoo, B. Das and B. K. Mishra, *Appl. Surf. Sci.*, 2014, 295, 115-122.